BULLETIN OF THE POLISH ACADEMY OF SCIENCES
TECHNICAL SCIENCES, Vol. 70(1), 2022, Article number: e140015
DOI: 10.24425/bpasts.2022.140015

Solar photovoltaic interconnected ZSI-unified power quality conditioner to enhance power quality

A. RAJA[1], M. VIJAYAKUMAR[2*], and C. KARTHIKEYAN[3]

[1] Electrical and Electronics Engineering Department, SSM College of Engineering, Kumarapalayam, Namakkal – 638 183, Tamilnadu, India
[2] Electrical and Electronics Engineering Department, K.S.R. College of Engineering, Tiruchengode, Namakkal – 637 215, Tamilnadu, India
[3] Electrical Department,Tamil Nadu Generation and Distribution Corporation Ltd., Erode – 638009, Tamilnadu, India

Abstract. In order to ensure that all the connected Equipment in the distribution network operates smoothly, the voltage stability of photovoltaic (PV) integrated distribution systems is very important. Sustaining the voltage profile when integrating PV is a particularly difficult issue. The primary goal of this article is to provide a consistent voltage profile to a sensitive load. A three-phase PV integrated distribution system has been chosen for investigation. An innovative feature of this system is that UPQC DVR and STATCOM systems are powered by Z-source inverters instead of traditional inverters. The ability to actively decouple power is the primary benefit of utilizing a Z-source inverter. The objective of the study effort is to use this new UPQC to synchronize a solar PV system with the distribution system. For the UPQC with battery energy storage system (BESS), the research study examines and develops the most appropriate control approach. A UPQC is a device that is used to integrate solar panels and improve the voltage stability of the distribution system. The prototype model is being developed, and the experimental findings confirm the main objective.

Key words: Z-source inverter; photovoltaic; power quality; unified power quality conditioner; total harmonic distortion.

1. INTRODUCTION

An electric utility must satisfy power quality requirements by supplying electricity at ratings of voltage and frequency. Power quality problems nowadays include reactive power consumption owing to poor power factor loads, the harmonic current burden from non-linear loads, including converters, battery chargers, mercury vapor lamps, and computers [1]. Furthermore, single-phase loads may cause an imbalance in the distribution supply load. In addition to being a sustainable energy source, solar photovoltaic systems are also pollution-free. Incorporating PV will decrease the need for traditional fuels as well as distribution system losses. Reactive power cannot be provided by a photovoltaic system since it lacks that capability. The energy industry urgently must take steps to address these power quality concerns. UPQC is a power quality compensation device that is commonly utilized in systems to enhance power quality [2, 3]. STATCOM and DVR are the two types of inverters that are included. The system must compensate dynamically for reactive power, and STATCOM is a great option for harmonic removal and active load compensation. The DVR is primarily used to reduce voltage sags and swells. This article discusses the integration of solar PV into the power system by using UPQC [4]. The quality of the power reflects the voltage quality and frequency stability. Even if the frequency of the Indian grid is steady, the voltage profile in certain places must be enhanced. It follows that if the voltage changes by one percent, the difference in power will be two percent of the impedance-type load.

Similarly, with a change in demand of about 5%, the frequency shift is approximately 1 Hz for the integrated Indian Grid system. If there is a deficit in the frequency, the output power of the lights and the induction motor will be impacted negatively. The power quality of low-tension voltages and currents in the power supply is governed by IEEE standard 1159 (1995). The permissible dip limits range from 10% to 90% and last for 0.01 sec to 0.06 sec, respectively. Temporary, immediate, and momentary categories are used in the dip categorization scheme. It is common for voltage to increase (swell) in other phases when an earth fault develops on one of the lines. The use of an energy storage device at the inverter input may also provide active power compensation. The traditional techniques of reactive power compensation include the use of fixed capacitors or reactors, controlled capacitors or reactors, static volt ampere reactive (VAR) compensators, tap-changing transformers, excitation control of generators, and other similar devices and methods. These approaches are susceptible to dynamic reactive power adjustment. Shunt reactors are used to reduce line overvoltage, whereas shunt-linked capacitors are utilized to boost voltage during periods of high system load. Typically, STATCOM injects reactive electricity into the grid with appropriate load compensation scheduling. Shunt capacitors and reactors are ineffective at sustaining voltage during dynamic load changes and are incapable of supporting or providing the necessary power. Additionally, if STATCOM is utilized in conjunction with a battery energy storage system (BESS), active power may be injected into the line [5, 6]. To ensure that the voltage at each node or bus in a power system remains stable, it is crit-

*e-mail: mvijayksrce@gmail.com

Manuscript submitted 2020-01-14, revised 2020-03-31, initially accepted for publication 2020-04-18, published in February 2022.

ical to balance the reactive power production and demand at that node or bus. If there is a mismatch, the voltage will fluctuate. In contrast to frequency, voltage is a local characteristic that must be investigated. When balancing reactive power, it is necessary to consider each node or bus. Aside from that, the voltage across a bus is inversely proportional to the fault level across that bus. The power system voltage profile is determined by the V-Q sensitivity [6,7]. To keep the voltage stable, it should be set to a positive value on all buses and nodes. The system enters voltage instability mode if the voltage is determined to be negative at any one of the nodes or buses. DVR will take care of voltage sag and swell issues with appropriate design and management strategies [8]. The study of the literature reveals that most proposals do not include the LCL filter, BESS, DVR, D-STATCOM, or UPQC design characteristics [9, 10]. Traditionally, grid-connected inverters have been used to integrate photovoltaic systems. The author of this study intends to close the gap by creating a novel UPQC that utilizes a Z-source inverter for both DVR and STATCOM integration of photovoltaic systems, along with the design of all required parameters [11]. The uniqueness is that a three-phase UPQC with ZSI for PV integration is suggested. The STATCOM absorbs the oscillatory component of active power and injects the PV source active power, the load total reactive power, and the system reactive losses. The design is cost-effective, considering the low DC link voltage, the low capacity of the BESS, the low voltage capacity of the photovoltaic system, and the limited capacity of the inverter switches. Our research laboratory develops and validates a prototype model of the UPQC utilizing a Z-source inverter and an FPGA controller.

2. Z-SOURCE NETWORK-BASED UPQC TOPOLOGY

The circuit design in Fig. 1 illustrates a three-phase UPQC system with a Z-source inverter. The power supply is a three-phase, 400 V system. The direct current (DC) link voltage is 600 V. To minimize total harmonic distortion (THD) in current and terminal voltage, the shunt STATCOM controller injects reactive current. With a power factor of unity, no reactive current from the source is required. To determine the reference current, the source should be made to provide only real power and losses [12,13]. The DVR is used to compensate for voltage sags and swells in the distribution network.

It is connected to three single-phase injection transformers that obtain their power from the series active power filter [14].

For the series APF injection transformer, the leakage reactance from each phase transformer is designed to be 0.01 p.u. to reduce voltage dips on the secondary side. With regard to the ZSI based PV-DVR, the injection transformer ratio has been adjusted at 1:2. The transformer ratio may be selected based on the injection capabilities of the device and the amount of injection voltage it can handle. Equation (1) shows the relationship between the two variables.

$$n_i = \frac{V_{\text{pri}}}{V_{\text{sec}}} = \frac{V_{\text{ZSI}}}{V_{Se}}, \tag{1}$$

Let, V_{Se} indicates the series APF output voltage, V_{sec} represents injection transformer secondary voltage and V_{ZSI} is the ZSI output voltage.

3. SPV-UPQC CONTROL SCHEME

Figure 2 shows the schematic diagram of the shunt and series compensator controller. For three-phase SPV-UPQC, an ESOGI-based control system is used in order to provide current compensation. As a feedback signal, the load current, as well as the compensatory currents, is evaluated. It is possible to assess the source reference current of specific phase currents in this voltage sensorless ESOGI control system. Consequently, three ESOGI controllers are used to obtain the reference values for the source currents [15, 16].

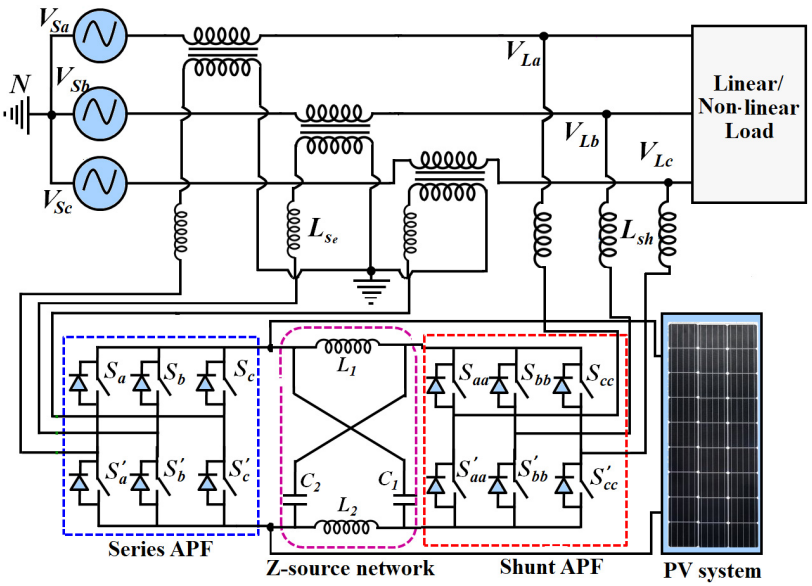

Fig. 1. Proposed solar photovoltaic supported UPQC topology

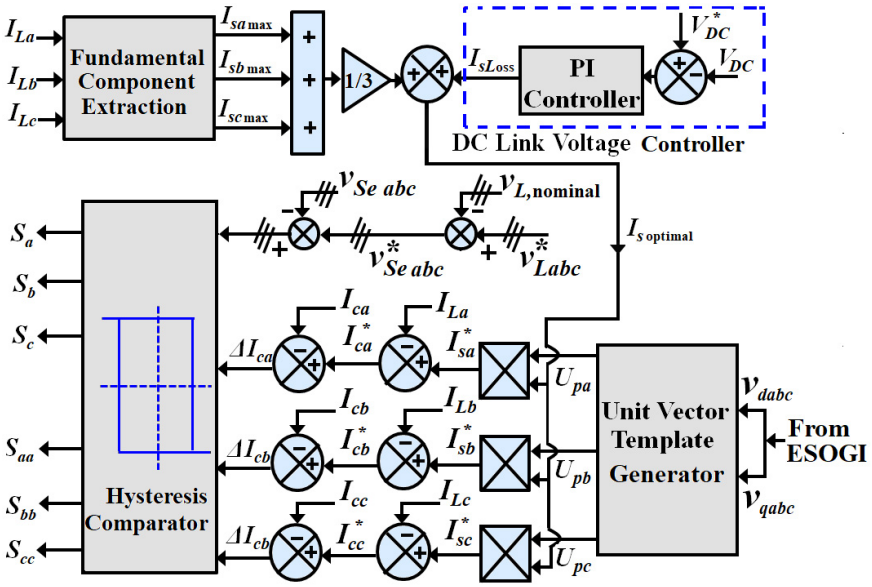

Fig. 2. Schematic diagram of shunt and series compensator

3.1. Extraction of the fundamental component

For the extraction of the basic component, there have been many SOGI-based methods developed in recent years [17, 18]. The issue with SOGI second output is that it is susceptible to DC as well as subharmonic distortion. In this case, SOGI signal identification is not adequate for the weak grid. The third integrator in the SOGI-based basic component extractor uses an enhanced SOGI-PLL to cancel the input DC component. This eliminates the issue. It has the potential to enhance performance without adding complexity. A third integrator uses the gain of k_{DC} to estimate the DC offset, which is subsequently removed from the input to enhance DC offset rejection. This results in the DC offset being computed by a third integrator, this time with a gain of k_{DC}, which is subsequently subtracted from the input signal in order to enhance DC offset rejection potential.

3.2. Computation of the shunt APF reference currents

Harmonic distortions are eliminated, and the reactive power of the system is balanced with the help of the reference current signal [19].

To explain why distorted voltages are created when the nonlinear load is connected to the system, consider how a nonsinusoidal load current travels via an impedance. The instantaneous load current is derived by Equation (2).

$$i_{Lx} = I_{Lx1}\sin(wt - \phi_{x1}) + \sum_{n=2}^{\infty} I_{Lxn}\sin(n\,wt - \phi_{xn}). \tag{2}$$

The basic real components of the source current are derived in equation (3) after mitigation.

$$I_{sxm} = |I_{Lx1}|\cos\phi_{x1}\,. \tag{3}$$

Variations in the DC-link voltage of ZSI are caused by losses in power electronic switches, losses in filter circuits, and load fluctuations. This controller is used to maintain the DC-link voltage of UPQC at a constant level relative to its reference value [20, 21]. If the system is properly balanced, the optimal source current value may be stated.

$$I_{s\,\mathrm{optimal}} = \left(\frac{I_{sa\max} + I_{sb\max} + I_{sc\max}}{3}\right) + I_{\mathrm{SLoss}}\,. \tag{4}$$

The switching loss current is represented by I_{SL}, and the optimum source current is represented by I_{sm}. The source current reference must be sinusoidal in order to properly adjust for variations in amplitude and phase with the ideal source current. Using equation (5), we can calculate the unit vectors

$$U_{px} = \frac{v_{dx}}{\sqrt{v_{dx}^2 + v_{qx}^2}}\,, \tag{5}$$

where x expresses the definite phase (a, b, or c). The inaccuracy in the DC-link voltage is derived at the nth sample moment.

$$V_{dc\,\mathrm{error}(n)} = V^*_{dc\,\mathrm{error}(n)} - V_{dc\,\mathrm{error}(n)}\,. \tag{6}$$

A prediction is made for the PI controller output at the nth instant of the sample period.

$$I_{\max(n)} = I_{\max(n-1)} - K_{P_{dc}}\left(V_{dc\,\mathrm{error}(n)} - V_{dc\,\mathrm{error}(n-1)}\right) + K_{I_{dc}}\,V_{dc\,\mathrm{error}(n)}\,. \tag{7}$$

Because of this, a unit template (U_{px}) is used that is in phase with the supply voltage to multiply the anticipated source current peak value [22]. Equation (8) calculates the real reference compensation current.

$$I^*_{ca} = I^*_{sa} - I_{La};\quad I^*_{cb} = I^*_{sb} - I_{Lb};\quad I^*_{cc} = I^*_{sc} - I_{Lc}\,. \tag{8}$$

When comparing the reference compensation currents with the actual compensation currents, it is possible to get an approx-

imation of the error signals. The compensating error signals are therefore obtained from the equation.

$$\Delta I_{ca} = I^*_{ca} - I_{ca}; \quad \Delta I_{cb} = I^*_{cb} - I_{cb}; \quad \Delta I_{cc} = I^*_{cc} - I_{cc}\,. \tag{9}$$

3.3. Computation of the series APF reference voltages

A series APF controller estimates the reference series APF voltages by comparing the load nominal voltage with the load-side voltages in the three phases [23].

$$V^*_{Sex} = V^*_{L\text{nominal}} - V_{Lx}\,. \tag{10}$$

The nominal value of load voltage is indicated by $V^*_{L\text{nominal}}$, the load-side voltage is indicated by V_{Lx}. The switching states for series APF are shown in Table 1.

Table 1
Switching states for series active power filter

	$V_{Sex} \geq V^*_{Sex} + h_1$	$V_{Sex} \leq V^*_{Sex} - h_1$
S_x	0	1
S'_x	1	0

The hysteresis band (h_1) has a value of 6.9 V.

4. VALIDATION THROUGH EXPERIMENTATION

Results from the experiments will illustrate the viability and effectiveness of the proposed control system and compensator. Figure 3 depicts a hardware prototype of the ZSI-UPQC. Xilinx SPARTAN 6 FPGA controller generates the pulse width modulation (PWM) signals in this experimental prototype. An analog to digital converter (ADC) and zero crossing detector (ZCD) use the decreased voltage from the step-down transformer. With the ZCD output, the 3-phase UPQC output voltage may be matched to the supply voltage for a perfect fit. Using the ADC digital output signal converted into an FPGA controller, the estimated magnitude of each phase voltage is determined. C and assembly language are used to program the UPQC control algorithm into the XC6SLX25 field-programmable gate array (FPGA). PWM pulses generated by the 3-phase voltage of ZSI and current are controlled by a UPQC control algorithm.

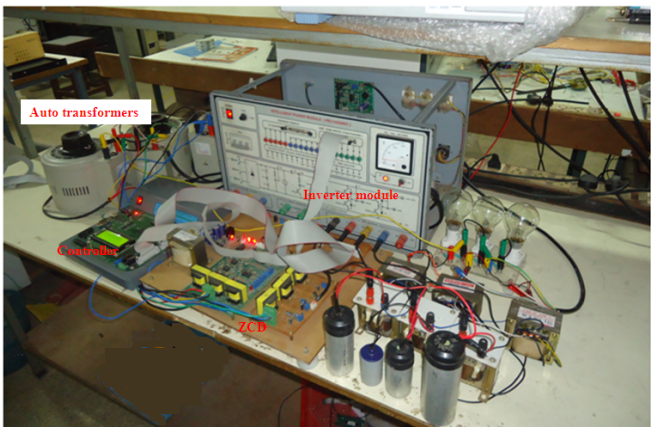

Fig. 3. ZSI-UPQC experimental set-up

The experimental research shows the outcomes before and after using the SPV-UPQC method. In a solar photovoltaic-based unified active power filter system, the following system parameters are used: system phase voltage = 230 V, DC-link voltage = 520 V, switching frequency = 10 kHz, shunt APF-filter: $L_f = 23$ mH, $R_f = 2.5\,\Omega$, filter (series APF): $L_{se} = 5$ mH, $C_{se} = 80$ µF. Studies have been performed using a range of distinct load circumstances, such as Equal source voltages and Equal loads, or Equal source voltages with unequal loads.

4.1. Balanced supply voltages and load currents

The SPV-supported ZSI-UPQC functionality is evaluated with balanced voltage and load current. The balanced voltage sag is used to measure voltage compensation. The injection transformer injects compensatory voltage when the SPV-UPQC detects a decrease in voltage. As can be seen in Fig. 4, before

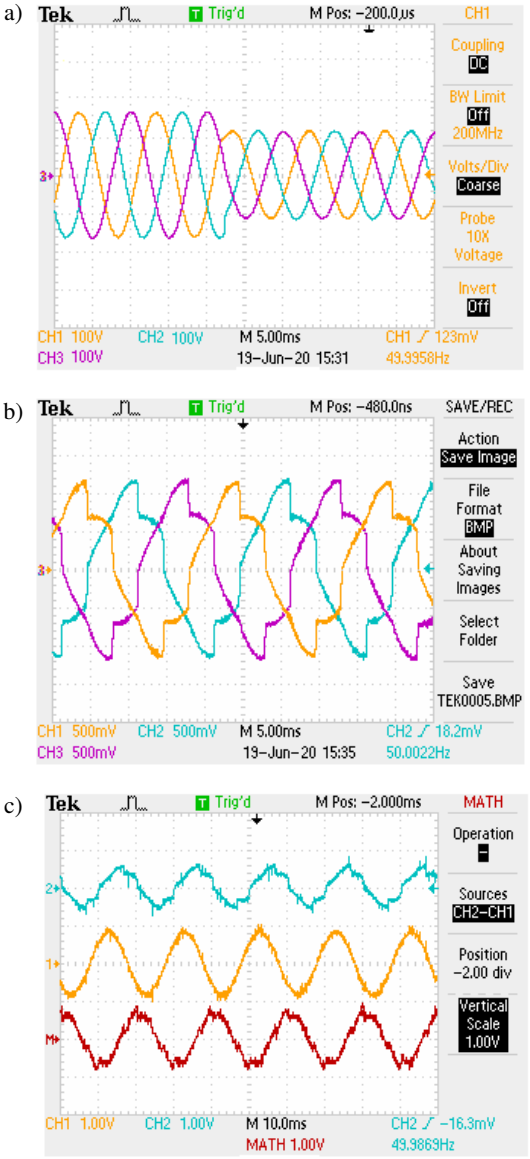

Fig. 4. Results from experiments with voltage and current kept balanced: a) voltage from the utility grid, b) connected load current, c) connected load current, current of the grid and compensation current

attaching the ZSI-based UPQC, the voltage of the utility grid, connected load current, and THD level of the balanced load current were all measured.

Figure 5 depicts the harmonics distortion level of the source current prior to attaching the solar photovoltaic assisted ZSI-UPQC.

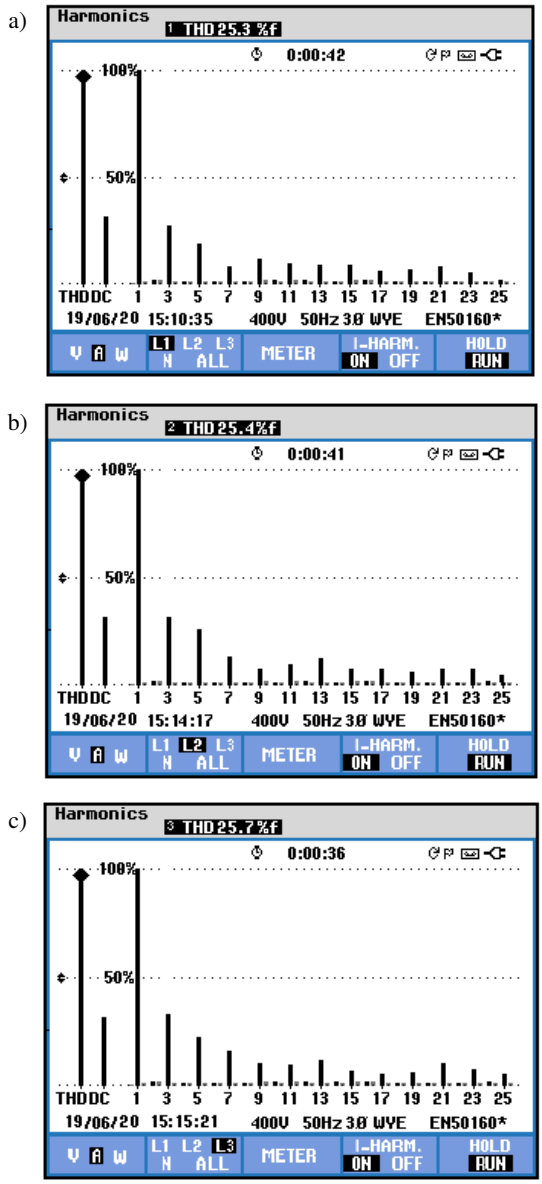

Fig. 5. Source current THD level before attaching solar photovoltaic powered by a ZSI-UPQC

Figure 6 depicts the source current after connecting the ZSI-UPQC, the injected voltage, the output voltage of the load, as well as the source current and voltage of the source.

Using an SPV-supported ZSI-UPQC, the harmonic distortion of the source current is shown in Fig. 7. Using a balanced load and balanced voltage, the proposed SPV-UPQC control system is evaluated for its performance. After adjustment, the source current harmonic content using the proposed approach is 1.2% when using the UPQC under these circumstances.

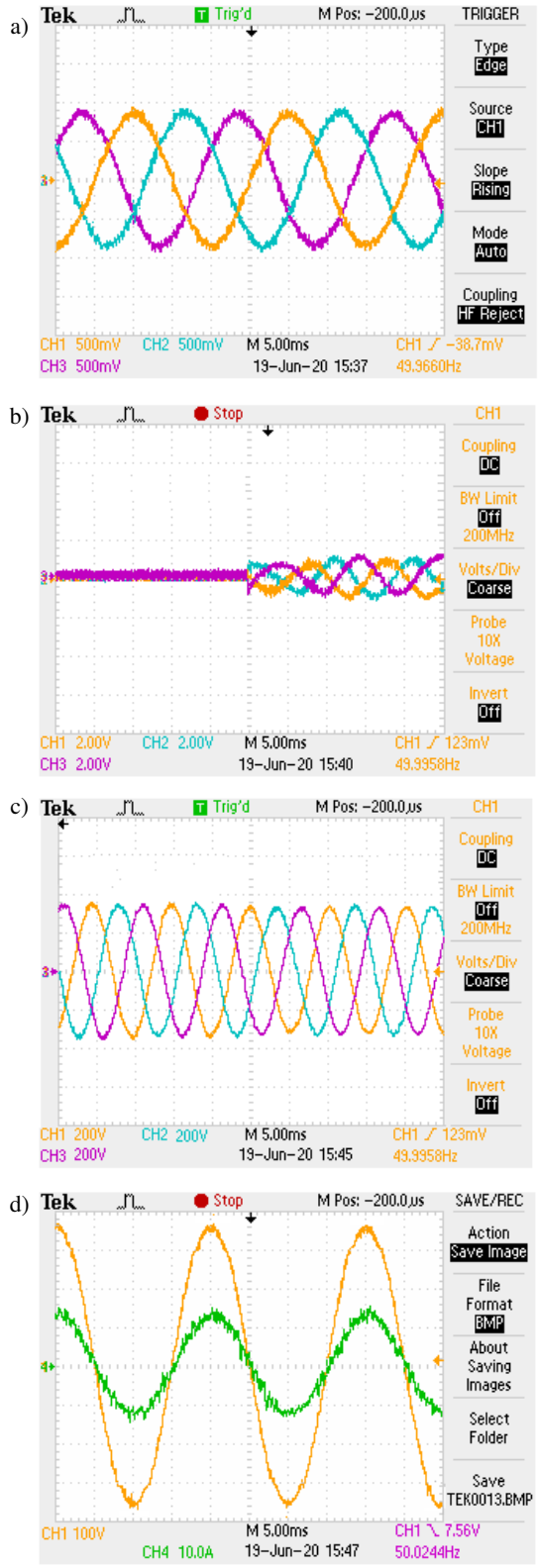

Fig. 6. Results from experiments conducted at steady voltage and current: (a) current from the utility grid, (b) voltage injected for compensation, (c) voltage at load terminal, (d) current from the grid and grid voltage

As shown in Fig. 8, the voltages of capacitors 1 and 2 and Z-source network output voltage.

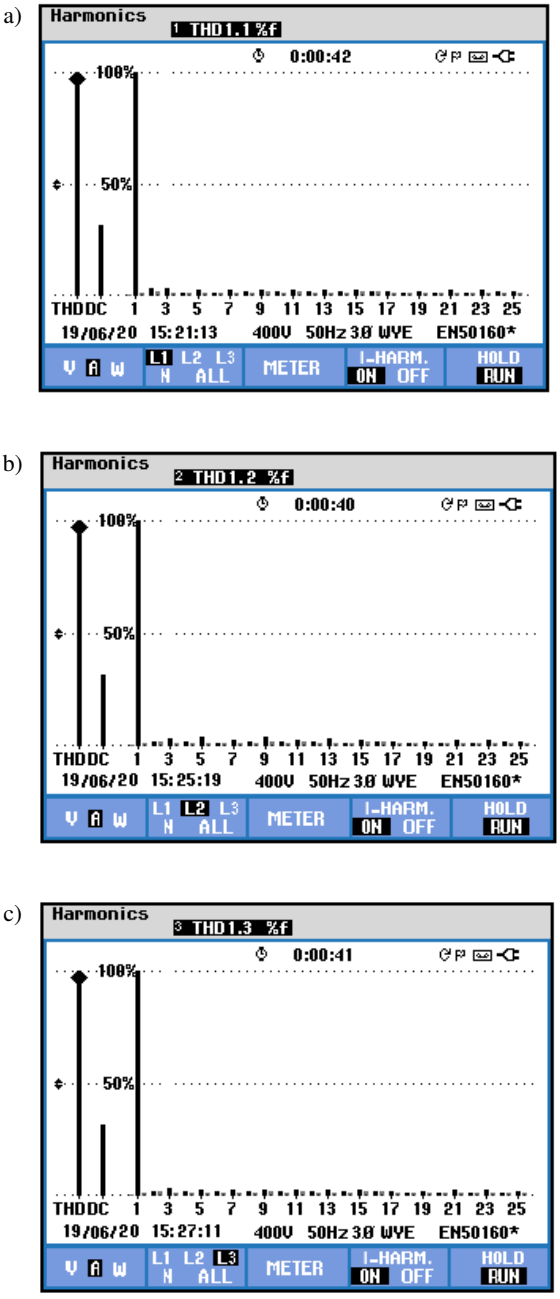

Fig. 7. Current THD before attaching ZSI-UPQC supported by solar photovoltaic

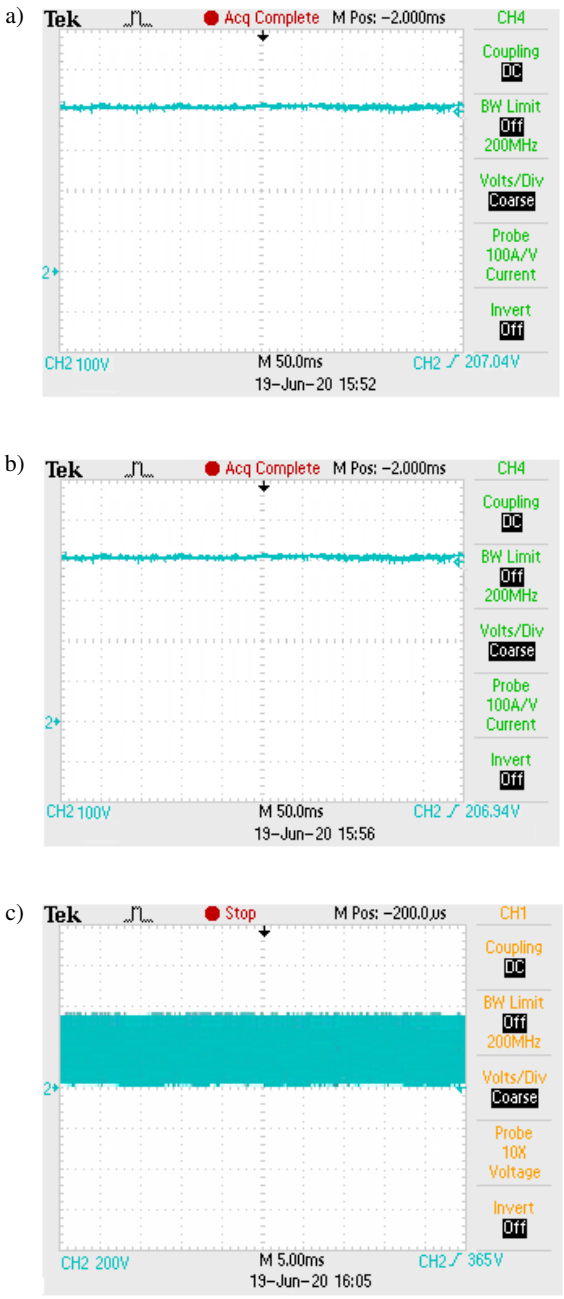

Fig. 8. a) capacitor 1 voltage, b) capacitor 2 voltage, c) Z-source network output voltage

4.2. Balanced voltages with unbalanced loads

Unbalanced load currents result when connecting single-phase rectifier circuits to three-phase lines. A ZSI-based UPQC is connected before the supply voltage, current, and harmonic current distortions are shown in Fig. 9. As a result of connecting ZSI-UPQC, Fig. 10 shows voltage injected for compensation, current from the utility grid, voltage at load terminal, and harmonics analysis. The findings of the experiments reveal that in three-phase four-wire electric power systems, a control strategy is used to reduce harmonic components and voltage distortion.

An unbalanced load is applied to the SPV-UPQC with the ESOGI control system to see how it performs under balanced voltage. After compensation, the source current harmonic content with the proposed approach is 1.2% when used with the UPQC in the experimental investigation using the recommended control system. Figure 11 displays the Z-source network voltage across the condensers and SPV array voltage.

Experiments at the same load are used to determine the efficacy of ESOGI control systems for UPQC. The level of source current harmonics before compensation is 25.2%, 25.7%, and 25.4%, while the level after compensation is 1.2%, 1.2%, and 1.1%. By removing the source voltage, it was possible to evaluate the voltage interruption compensation during experimental validation.

a)

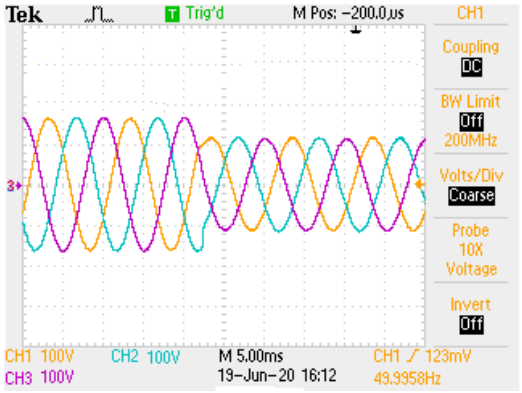

b)

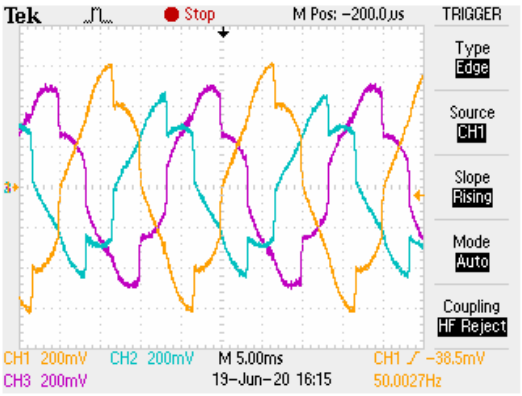

c)

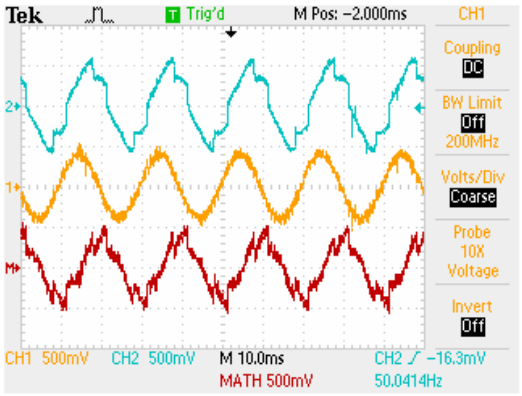

d)

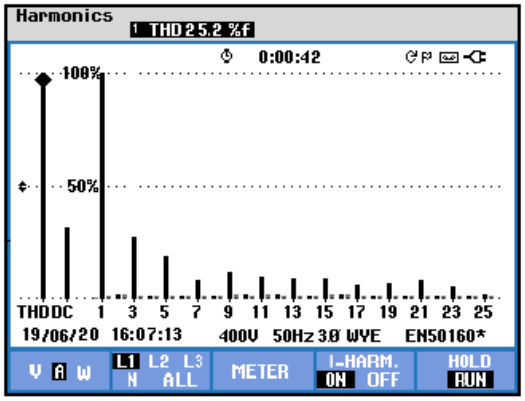

Fig. 9. Results from experiments with balanced voltages and unbalanced loads: a) voltage from the utility grid, b) connected load current, c) connected load current, current of the grid, and compensation current, d) harmonic distortion results

a)

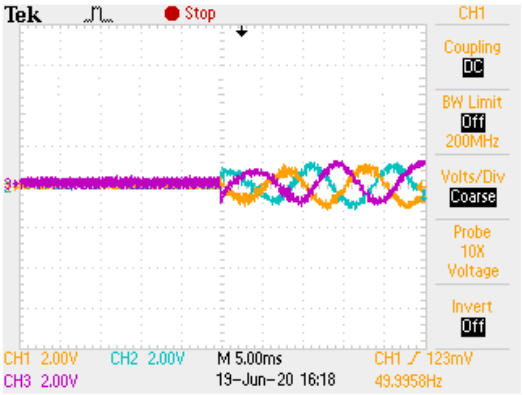

b)

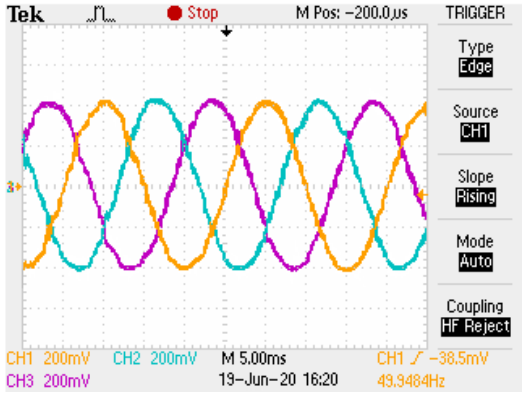

c)

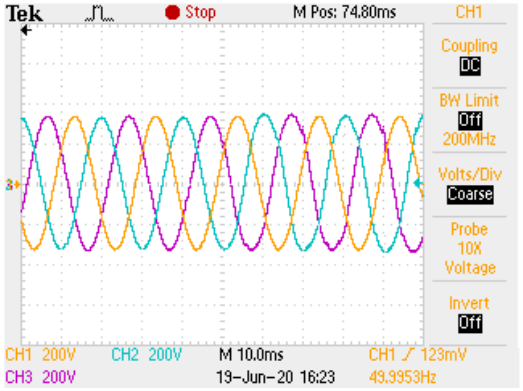

d)

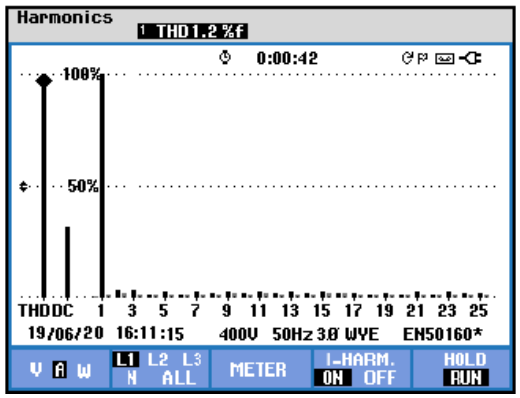

Fig. 10. Results of experiments: a) voltage injected for compensation, b) current from the utility grid, c) voltage at load terminal, d) harmonic distortion results

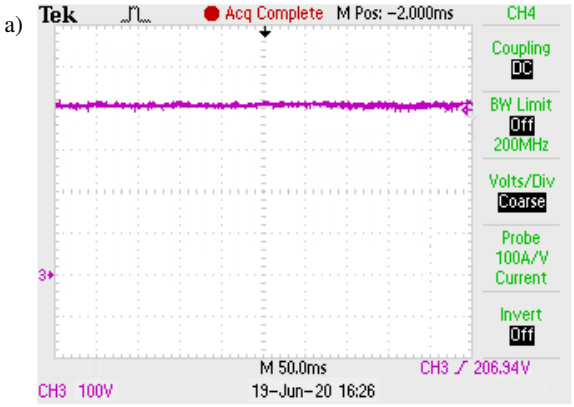

Fig. 11. a) Z-source network voltage across the condensers and b) SPV array voltage solar photovoltaic array voltage

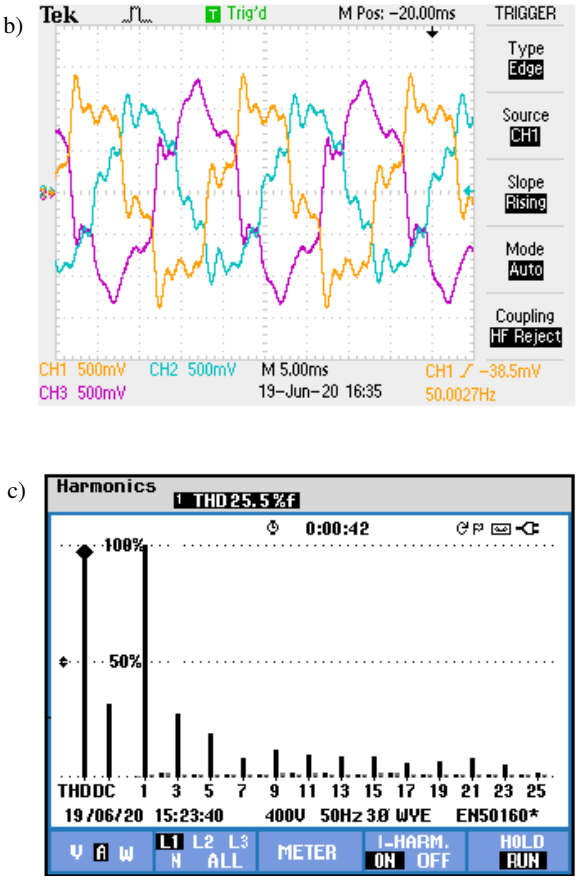

Fig. 12. a) voltage from the utility grid, b) connected load current, c) harmonic distortion results

4.3. Unbalanced voltages with unbalanced loads

It is necessary to conduct the experimental test with unbalanced voltages and uneven load currents in order to get reliable results. The imbalanced voltage sag and swell are used in order to evaluate the voltage compensation. The injection transformer injects compensating voltage to make up for the voltage loss that was identified by the SPV-UPQC. Figure 12 depicts voltage from the utility grid, connected load current harmonic distortion results.

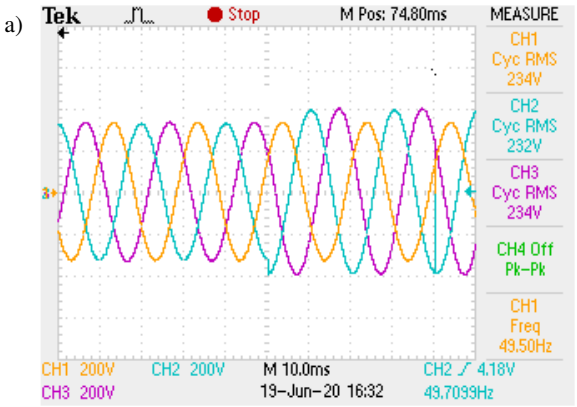

Fig. 12a

Figure 13 depicts the injected series APF voltage, voltage at load terminal, current from the utility grid, and the harmonic distortion after the solar photovoltaic unified active power filter connection.

When source currents are not compensated, their total harmonic distortion in percentage is 25.5, 25.3, and 25.6, respectively. When compensation is applied, the THD of source currents is decreased to 1.2, 1.2, and 1.3. Table 2 demonstrates the results of harmonic distortions. The level of measuring THD is extremely low and suited for grid-connected applications as per IEEE-519-1992 Standard.

Table 2
Results of harmonic distortions

Phase	Case study 1		Case study 2		Case study 3	
	Before compensation	With compensation	Before compensation	With compensation	Before compensation	With compensation
	Current THD (%)					
A	25.3	1.1	25.2	1.2	25.5	1.2
B	25.4	1.2	25.7	1.2	25.3	1.2
C	25.7	1.3	25.4	1.1	25.6	1.3

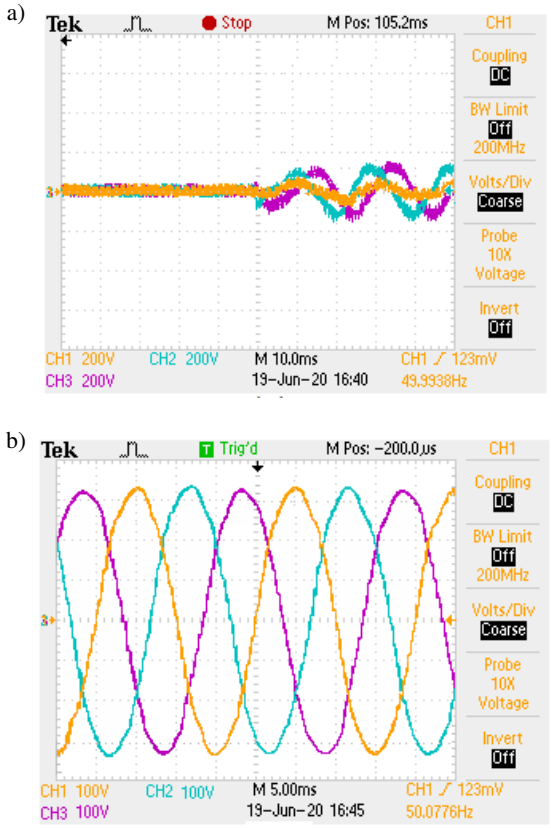

Fig. 13. Findings from experiments conducted at voltages that were not balanced and with loads that had uneven loads: a) injected series APF voltage, b) voltage at load terminal, c) current from the utility grid, d) harmonic distortion results

5. CONCLUSION

ZSI-UPQC with enhanced SOGI control is used in this study to integrate solar PV into the grid in the face of severely non-linear load, which is discussed in detail in the paper. SPV interfaced three-phase four-wire ZSI-UPQC uses this technique to compensate for power quality issues in the electric distribution networks. With the SPV power generating technology, voltage and current instability in the distribution networks may be reduced in the long run. SPV power production systems may share and store any extra power they create in the form of battery-powered energy storage devices. Regardless of the scenario, the SPV power system ensures that clean power is delivered to the load consistently. Under dynamic source and load conditions, our ESOGI control algorithm efficiently compensated for harmonic distortions, voltage, and current. An experimental model is used to evaluate the whole system, and THD analyses are carried out in both steady and dynamic circumstances. In the experiments, the non-linearity of the load was successfully compensated for using the proposed approach. It also integrates the PV system easily into the grid while creating little grid distortion with respect to the proposed technique.

REFERENCES

[1] I.P.W. Group *et al.*, "Recommended practice for monitoring electric power quality", *Technical report, Draft 5*, 1994.

[2] P.K. Ray, S.R. Mohanty, and N. Kishor, "Classification of powerquality disturbances due to environmental characteristics in distributedgeneration system", *IEEE Trans. Sustain. Energy*, vol. 4, no. 2, pp. 302–313, 2013.

[3] B. Singh, A. Chandra, and K. Al-Haddad, *Power Quality Problems and Mitigation Techniques*. Chichester, West Sussex, United Kingdom: John Wiley & Sons Inc, 2015.

[4] P. Chaudhary and M. Rizwan, "Voltage regulation mitigation techniques in distribution system with high pv penetration: A review", *Renew. Sustain. Energy Rev.*, vol. 82, pp. 3279–3287, 2018.

[5] P.K. Ray, S.R. Mohanty, N. Kishor, and J.P.S. Catalao, "Optimal feature and decision tree-based classification of power quality disturbances in distributed generation systems", *IEEE Trans. Sustain. Energy*, vol. 5, no. 1, pp. 200–208, Jan 2014.

[6] A. Kasprowicz, "Induction generator with three-level inverters and LCL filter connected to the power grid", *Bull. Pol. Acad. Sci. Tech. Sci.*, vol. 67, pp. 593–604, 2019.

[7] T. Koroglu, A. Tan, M.M. Savrun, M.U. Cuma, K.C. Bayindir, and M. Tumay, "Implementation of a Novel Hybrid UPQC Topology Endowed With an Isolated Bidirectional DC–DC Converter at DC link", *IEEE Trans. Emerg. Sel. Topics Power Electron.*, vol. 8, no. 3, pp. 2733–2746, 2020.

[8] W.U. Tareen, S. Mekhilef, M. Seyedmahmoudian, and B. Horan, "Active power filter (apf) for mitigation of power quality issues in grid integration of wind and photovoltaic energy conversion system", *Renew. Sustain. Energy Rev.*, vol. 70, pp. 635–655, 2017.

[9] S. Patra, N. Kishor, S. R. Mohanty, and P.K. Ray, "Power qualityassessment in 3-phase grid connected pv system with single and dual stage circuits", *Int. J. Electr. Power Energy Syst.*, vol. 75, pp. 275–288, 2016.

[10] W. Sleszyński, A. Cichowski and P. Mysiak, "Current harmonic controller in multiple reference frames for series active power filter integrated with 18-pulse diode rectifier", *Bull. Pol. Acad. Sci. Tech. Sci.*, vol. 66, pp. 699–704, 2018.

[11] A. Sangwongwanich, Y. Yang, D. Sera, H. Soltani, and F. Blaabjerg, "Analysis and modeling of interharmonics from grid-connected photovoltaic systems", *IEEE Trans. Power Electron.*, vol. 33, no. 10, pp. 8353–8364, 2018.

[12] M. Vijayakumar and S. Vijayan, "Extended reference signal generation scheme for integration of unified power quality conditioner in grid-connected photovoltaic system", *Electr. Power Compon. Syst.*, vol. 43, no. 8–10, pp. 914–927, 2015.

[13] A.G. Shaik and O.P. Mahela, "Power quality assessment and event detection in hybrid power system", *Electr. Power Syst. Res.*, vol. 161, pp. 26–44, 2018.

[14] P. Miska and A.A. Kumar, "Performance of DSTATCOM Control Schemes for Voltage Quality Improvement", *Aust. J. Basic Appl. Sci.*, vol.10, no. 15, pp. 315–324, 2016.

[15] S.S. Pawar, A. Deshpande, and M. Murali, "Modelling and simulation of dstatcom for power quality improvement in distribution system using matlab simulink tool", in *Energy Syst. and Applications, 2015 International Conference on, IEEE*, pp. 224–227, 2015.

[16] M. Kesler and E. Ozdemir, "Synchronous-Reference-Frame-Based Control Method for UPQC Under Unbalanced and Distorted Load Conditions", *IEEE Trans. Ind. Electron.*, vol. 58, no. 9, pp. 3967–3975, Sept. 2011.

[17] Z. Xin, X Wang, Z. Qin, P.C. Loh, and F. Blaabjerg, "An Improved Second-Order Generalized Integrator Based Quadrature Signal Generator", *IEEE Trans. Power Electron.*, vol. 31, no. 12, pp. 8068–8073, June. 2016.

[18] M. Bobrowska-Rafal, K. Rafal, M. Jasinski, and M.P. Kazmierkowski "Grid synchronization and symmetrical components extraction with PLL algorithm for grid connected power electronic converters – A review", *Bull. Pol. Acad. Sci. Tech. Sci.*, vol. 59, no. 4, pp. 485–497, 2011.

[19] S.W. Kang, and K.H. Kim, "Sliding mode harmonic compensation strategy for power quality improvement of a grid-connected inverter under distorted grid condition", *IET Power Electron.*, vol. 8, no. 8, pp. 1461–1472, 2015.

[20] Y.Y. Kolhatkar and S.P. Das, "Experimental investigation of a single phase upqc with minimum va loading", *IEEE Trans. Power Deliv.*, vol. 22, no. 1, pp. 373–380, 2006.

[21] A.K. Maity, R. Pratihar, S. Sadhu, and S. Dalai, "Biogeography based PI controller for unified power quality conditioner", 2016, *IEEE First International Conference on Control, Measurement and Instrumentation (CMI)*, 2016, pp. 254–258.

[22] S.K. Dash, S. Mishra, and P.K. Ray, "Photovoltaic tied unified power quality conditioner for mitigation of voltage distortions", 2016, *International Conference on Computer, Electrical & Communication Engineering (ICCECE*), 2016, pp. 1–5.

[23] K. Muthuvel and M. Vijayakumar, "Solar PV Sustained Quasi Z-Source Network-Based Unified Power Quality Conditioner for Enhancement of Power Quality", *Energies*, vol. 13, no. 10, p. 2657, 2020.